

## Improving Accuracy and Increasing Resolution of the World and Local DEMs through Data fusion

By:

**Assoc. prof. . Maher M. Amin**  
Assoc. Proff. of Geodesy  
Shoubra Faculty of Engineering

**Dr. Saadia M. El-Fatiry**  
Lecturer of Geodesy  
Shoubra Faculty of Engineerin

**ENG.Nasr Mohammady Saba**  
M.sc. student, Department of Surveying  
Shoubra Faculty of Engineering

### ملخص البحث

تعد نماذج الارتفاعات الرقمية العالمية والمحلية أحد أهم وسائل الحصول علي بيانات الارتفاعات. تنتج تلك النماذج بطرق وتقنيات مختلفة تؤدي الي تباينها في الدقة والتفاصيل, يهدف البحث الي دمج البيانات الناتجة من بعض تلك المصادر العالمية والمتمثلة في نماذج ASTER و SRTM وكذلك المحلية الناتجة من الخرائط الطبوغرافية ذات مقياس الرسم 1:50,000 لانتاج نموذج رقمي اكثر دقة وتفصيلا. وقد تم اختيار منطقة شمال وادي النيل كمئنة للدراسة بين خطي عرض (28°, 31.5°) وخطي طول (31.5°, 30°) بمساحة (60,000) كيلو متر مربع. تم تقييم الدقة الرأسية للنماذج الثلاث باستخدام عدد من الثوابت الأرضية. واتضح وجود تقارب في الدقة بين نموذج SRTM والنموذج المحلي بينما قلت كثيرا دقة نموذج ASTER. اتضح أيضا وجود ازاحة رأسية لنموذج ASTER عن كلا النموذجين الاخرين. لذلك تم الاستعانة بشبكة الطرق الموجودة علي الخرائط الطبوغرافية للكشف عن وجود ازاحة افقية لهذا النموذج من عدمه و حساب الازاحة الرأسية لنفس النموذج منسوبة الي نموذج SRTM والعمل علي تصحيحهما. وبعد ازالة الازاحة الافقية والرأسية لهذا النموذج والتأكد من أن الثلاث نماذج اصبحت في حالة تطابق أفقي وتقارب رأسي, تمت عملية الدمج بين كل نموذجين علي حدة وبين النماذج الثلاث في ان واحد واستخدمت تقنية (low pass filtering) لعمل تجانس بين البيانات المدمجة. ومن ذلك أستخلصنا ان دقة النماذج المدمجة تحسنت كثيرا بمقارنتها بدقة النماذج الأولية قبل الدمج وخصوصا في حالة دمج الثلاث نماذج معا, هذا بالاضافة ان النموذج المدمج اصبح يمتلك نفس القدرة التحليلية لنموذج ASTER (30 m) غير انه اعتمد في انتاج تفاصيله علي عدد اكثر من نقاط الارتفاع مقارنة بأي من النماذج الثلاث قبل الدمج. وحيث كانت قيمة الجزر التريبيعي لمتوسط الاخطاء لهذا النموذج المدمج هي 4.55 م لذا فانه يصلح لكثير من الاعمال الهندسية بما فيها انتاج خرائط طبوغرافية بمقياس رسم 1:50,000

## 1 ABSTRACT

ASTER and SRTM are two possible world sources for DEM covering the whole country. On the other hand, topographic maps of different scales are considered as local and reliable sources of DEM data. In this paper fusion among these DEMs is applied to produce a more accurate and detailed DEM for the studying area. First, ASTER DEM was co-registered to the horizontal coordinate system of the local DEM based on road intersection as distinct features. Second, the ASTER DEM was shifted vertically to the mean elevation of the SRTM. Several strategies integration among the three DEMs had been made. Low pass filtering technique through surfer software is applied to the fused DEMs to remove the erroneous frequency components from them. Fusion and filtration processes made an enormous improvement especially in the case of integrating the data of the three DEMs. Since the fusion was applied to 30m, 90m and 200m resolution input DEMs, the fused DEM had the least grid size of resolution. The approach showed improved DEMs accuracy and completeness while maintaining the highest resolution of the input DEMs. The resulted RMSE of the fused DEM was 4.55m, which make it useful for many applications as producing topographic maps of scale 1:50,000.

## 2 INTRODUCTION

As the numbers of satellite-based DEM sources increases, there is a strong need for careful accuracy assessment of each available DEM. Since different satellite sensors use different wavelength regions and/or viewing geometries, data collected by these sensors may provide slightly different but complementary information [10]. Availability of DEMs from multiple sources and their complementary nature open the opportunity to fuse multi-source DEM products to generate a value-added product that is more complete, accurate and reliable. Several studies have been carried out to address this need. The synergy between stereo optical DEM and Radar DEM in the spatial frequency domain was used to filter out the error prone components of SPOT DEM and ERS-1 DEM. The fused DEM was improved in terms of Root Mean Squared Error (RMSE) and error distribution [6]. In another study, a DEM fusion process

was introduced, which took advantage of the synergy between InSAR DEM and stereo optical DEM generation, by weighting the height values in both DEMs according to the estimated error. The study tested the fusion approach with SPOT and ERS DEMs having very different accuracies [7]. Nonetheless, these multi-sensor, multi-technology DEM fusion techniques have not dealt with possible voids, and thus fusion performance may be disgraced if a substantial number of voids exist in one of the input DEMs. Another study used optical stereoscopic and InSAR techniques to treat the Indian Remote Sensing (IRS-1C) PAN stereo and European Remote- Sensing Satellite (ERS-1/2) tandem data, respectively to generate DEMs [14]. They compared the DEMs and fused them by replacing the voids of one DEM with data from the other DEM. Another combination technique had been made between SRTM and ASTER DEMs to remove the voids of SRTM DEM and used the resulting DEM to derive glacier flow in the mountains of Bhutan [9]. In our case the newer world DEMs ASTER and SRTM dataset beside a local DEM produced from topographic maps of scale 1:50,000 were used in a fused technique to produce a complete, more accurate and much reliable fused DEM.

### 3 Study Area and Used Data

The study area is located northern Nile Valley. It has a rectangle shape and extends from 30° E to 31.5° E and from 28° N to 31.5° N. The total area is about 60,000 km<sup>2</sup> (160 km by 380 km). It contains some mountains with summits reaching up about 453 meters above sea level, and some valleys with depression of about 50 meters below sea level. The northern and central part of this region is completely flat while the desert occupies most of the remaining region. Figure (1) shows the extensions of the study area. The available data in this research are 90 m spatial resolution SRTM DEM, a 30 m spatial resolution ASTER DEM and a 200 m spatial resolution local DEM produced from topographic maps of scale 1:50,000. The local DEM was generated through the process of digitizing contours and the spot elevations of a 64

sheet maps covering the whole subject area. The topographic maps were obtained from the military survey authority, where, a number of 950 ground control points (GCPs) were available in the study area and the final validated number of such ground control points was 705.

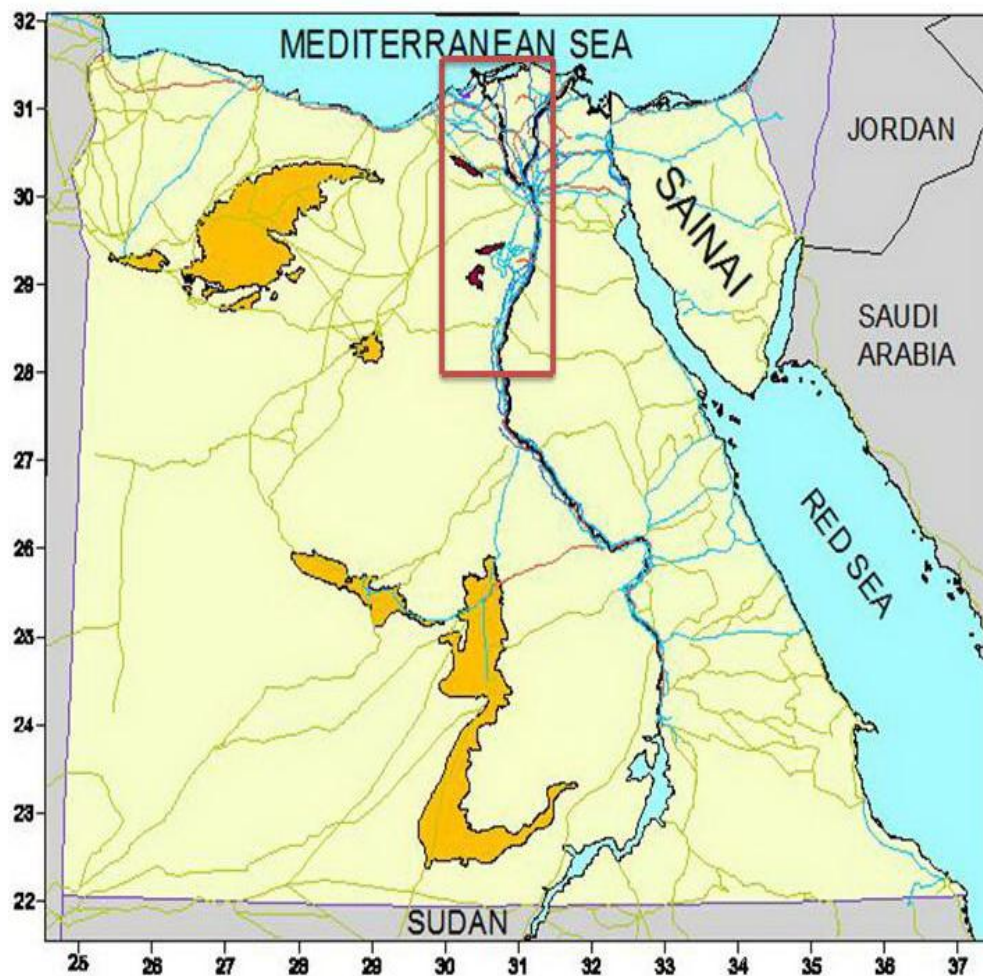


**Figure (1):** The extension of the study area.

These points were utilized as a reference data for the purpose of the evaluation process of the DEMs accuracy. The ASTER DEMs have a worldwide vertical RMSE of 10–50 m [11]. Regarding SRTM DEMs, the mission expected worldwide vertical RMSE of 10 m [14]. However, studies in mountainous regions revealed relatively

larger RMSE values in the range of 20–36 m [15]. Expected accuracy of DEM generated from topographic maps reaches half of the contour interval [2 and 3].

### **3.1 Creation of local DEM from Topographic Maps of Scale 1: 50,000**

The data set used for generating the local DEM from topographic maps were a digital contour and spot elevations data obtained from digitizing a number of 64 sheets of topographic maps of scale 1:50,000. The digitized contours and spot elevations were then used in an interpolation and gridding processes to gain a continuous surface of the terrain of the study area, where, interpolation is the mathematical tool used for determining intermediate unknown value between fixed known values or rate of surface change [18]. The institution of the local DEM is therefore, passes through several phases; data capture represented in map scanning and preparation, digitizing process ( raster to vector conversion), data filtering, and finally data conversion. The outcome of all the previous processes was an ASCII file that included 1435372 elevation points spreaded out over the whole study area , with an average density of 25 elevation points / km<sup>2</sup>. Consequently, a grid size of 200 meters was made based on the obtained density. Surfer software was then utilized for DEM creation through a gridding process in which all the irregular scattered points are set in a regular pattern of rectangular grid form. The obtained file after gridding is denoted as the local DEM.

### **3.2 ASTER and SRTM Digital Elevation Data**

Advanced Spaceborn Thermal Emission and Reflection Radiometer (ASTER) is a system based on a spaceborn earth observing optical instrument. ASTER Global Digital Elevation Model (ASTER GDEM) is a joint product developed and made available to the public by the Ministry of Economy, Trade, and Industry (METI) of japan and the United States National Aeronautics and Space Administration (NASA). The ASTER GDEM is the only DEM that covers the entire land surface of the earth at high

resolution; it covers the land surface between  $83^{\circ}\text{N}$  and  $83^{\circ}\text{S}$ . The ASTER GDEM is in a Geo TIFF format with geographic latitudes and longitudes and with 1 arc second (30m) grid of elevation postings. It is referenced to WGS84/EGM96 geoid [8]. Shuttle Radar Topography Mission (SRTM) was a single pass, synthetic aperture radar interferometry (InSAR) campaign conducted in February 2000. For the first time a global high-quality DEM was achieved with a grid resolution of 1 arc Sec (30m) and 3 arc Sec (90 m, free availability) covering the Earth's area between  $60^{\circ}\text{N}$  and  $54^{\circ}\text{S}$  [17]. It is referenced to the WGS84 datum. ASTER and SRTM were first downloaded from their website. Global Mapper software was then used to subset the DEMs relevant to the study area. Also a transformation from WGS84 to Helmert 1906 as adopted datum in Egypt had been done. The frame of reference of the study area was then converted from geodetic coordinates to map coordinates in the ETM system as the adopted projection in ESA. Table (1) shows some statistical information of the elevation data of the local and world DEMs.

**Table (1) :** Statistical of the three DEMs.

DEM	Z (elevation), m			Total No. of elevation points	Point density/ km <sup>2</sup>	Slope % Min- Max	Grid size (m)
	Min.	Max.	Mean				
Local DEM	-53	453	111	1,435,37	25	0 - 45	200
SRTM DEM	-52	435	96	6,886,88	123	0 - 11	90
ASTER DEM	-105	458	74	67,193,2	1109	0 - 78	30

#### 4 Accuracy Study of Used DEMs

RMS was used to assess the accuracy of interpolated DEMs elevations, it is the most widely used statistic as a measure of accuracy [5]; it measures the dispersion of the frequency distribution of deviations between the actual values and the estimated value. The RMS error characterizes the interpolation accuracy of the relevant points as well as the accuracy of the relevant models. The accuracy of DEM must be tested using points with known elevations (actual heights) i.e. ground control points (GCPs). The relevant

points, interpolated from the DEMs, are compared with the elevations of these GCPs, and RMS of elevation differences is estimated as:

$$\mathbf{RMS} = \sqrt{\frac{\sum(z_i - z'_i)^2}{n}} \quad (1)$$

Where,  $n$  is the number of check points,  $z_i$  is the original or known elevation,  $z'_i$  is interpolated elevation from the DEM. The elevation difference in each of the three DEMs is calculated at all the specific GCPs in order to verify DEMs accuracies. The reference data were filtered from gross errors. This step is very important to ensure that the input data has the optimum quality [1], which is essential for accuracy assessment. In that regard, all GCPs were subjected to a validation process that aimed to filter out any data element. lacking a minimal level of reliability. For any GCPs has differences (in the three models) exceeding 3 times the RMSE values is to filtered out. Figure (2) shows the distribution of these ground control points over the whole terrain. Table (2) show the statistics of the three DEMs. In the three DEM models,

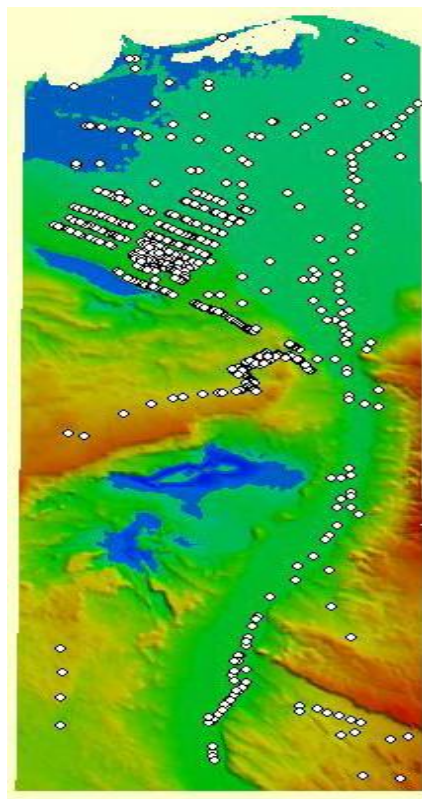


**Figure (2):** The distribution of GCPs over the whole terrain.

**Table (2):** Statistics of the elevation differences among the three DEMs and GCPs.

DEMs	Z- difference, m			No of check points	RMSE (m)
	Min.	Max.	Mean		
Local DEM	-16.62	20.12	0.04	705	4.85
SRTM DEM	-14.02	19.92	1.80	705	4.72
ASTER DEM	-14.45	34.59	12.55	705	14.53

The investigation of table (2) and the behaviour of elevation data reveals that, the difference between the elevations of the ground control points and the elevations of the related points at the three DEMs suffer from shifts. These shifts represented by the mean of elevation differences between the GCPs elevations and the elevations of relevant points values at each DEM. Therefore the DEMs elevations are shifted by equivalent values. The statistics of the DEMs were recalculated and the results are presented in table (3).

**Table (3):** Statistics of the elevation difference among the three DEMs over the whole terrain after shift elimination.

DEMs	Z- difference, m			No of check points	RMSE(m)
	Min.	Max.	Mean		
Local DEM	-16.58	20.16	0.0	705	4.85
SRTM DEM	-15.82	18.12	0.0	705	4.33
ASTER DEM	-26.80	22.24	0.0	705	7.33

From the above table it is clear that the RMSE were improved especially regarding ASTER DEM which improved by 49.5 % after the elimination of the vertical shift. Large shift of ASTER DEM may be due problems in the orientation of its data collecting sensor in addition to the inaccurate GCPs used by the USGS used in producing that DEM [12].

## 5 DEM Fusion

Before applying fusion process, the three DEMs are be related to the same horizontal position and a unique reference vertical datum. In other words, The co-registration of ASTER DEM is essential to enforce that DEM to coincide with the other two DEMs ( SRTM and local DEM). This is done by correcting ASTER horizontal positions related to the topographic maps (local DEM) based on a number of 6 main road intersection points that were digitized from topographic maps. These main roads intersections are clearly visible on the ASTER DEM due to its good resolution. The vertical displacement of the ASTER versus SRTM DEM has been removed. The ASTER DEM was thus transferred to the vertical and horizontal coordinate systems of the SRTM and the local DEM respectively, which was necessary to prepare the three DEMs related to a common reference surface (datum) before applying the merger process. Figure (3) shows the horizontal shift, existing between ASTER and the local DEM represented in road networks. As shown in figure (3), the crossings of the roads marked by circles are the points used to co-register the ASTER DEM. figure (3A) represents the network before co-registered and figure (3B) represented the network after the co-registration. The horizontal shift components between the ASTER and local DEM were found to be:  $dx = -87$  m,  $dy = -71.7$  m. The accuracy of this DEM had been improved by 3% after eliminating these horizontal shift component as shown in table (4). The vertical shift (DZ) between the ASTER DEM and SRTM DEM was calculated and found to be 10.3 m. The statistics were recalculated after correcting ASTER DEM ( horizontally and vertically) and presented in table (5). Figure (4-A) shows a Profile of ASTER, SRTM and local DEM along easting (latitude 28) as an example of the original case of DEMs. As shown from this figure, the ASTER DEM profile is in a downward with

respect to the other two DEMs profiles, while after co-registration, ASTER DEM profile in figure (4-B) is seems to be closed to the two profiles.

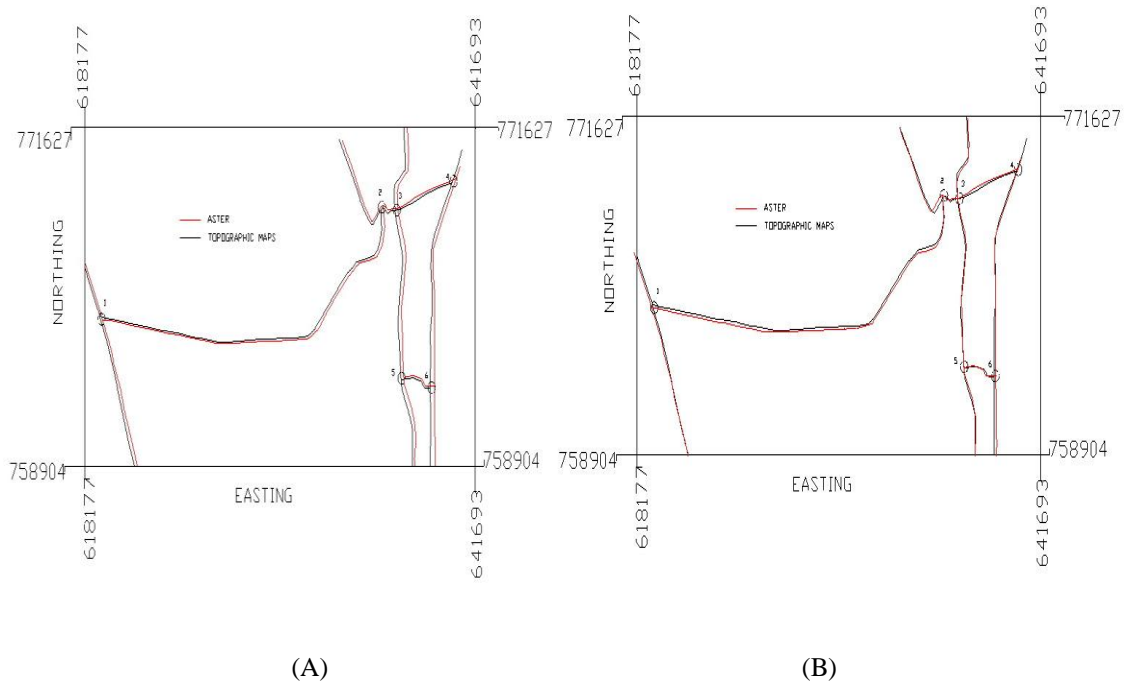


**Figure 3:** Roads networks digitized from topographic maps and ASTER DEM; A: Before co-registration, B: After co-registration.

**Table (4):** Statistics of the ASTER versus GCPs after horizontal shift elimination.

DEMs	Z- difference, m			No of check points	RMSE(m)
	Minimum	Maximum	Mean		
ASTER DEM	-20.35	24.75	12.05	705	14.05

**Table (5):** Statistics of the ASTER versus GCPs after horizontal and vertical shift elimination.

DEMs	Z- difference, m			No of check points	RMSE(m)
	Minimum	Maximum	Mean		
ASTER DEM	-24.28	25.07	1.85	705	7.46

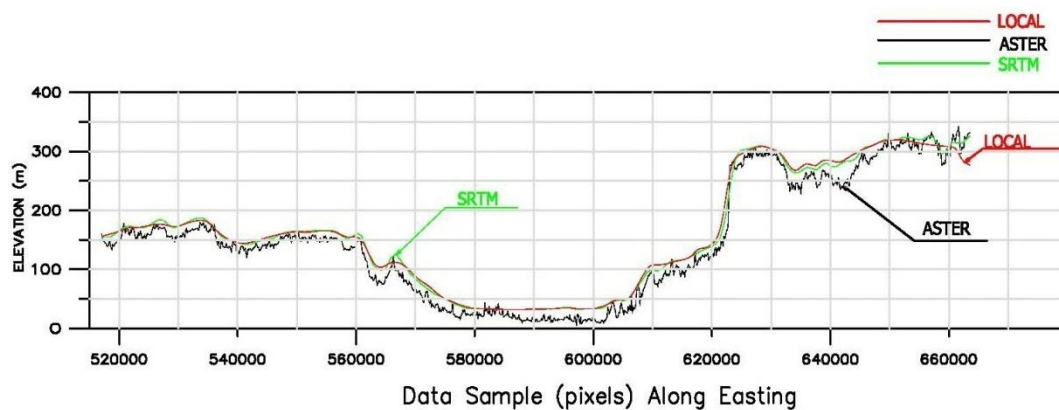


FIG:A

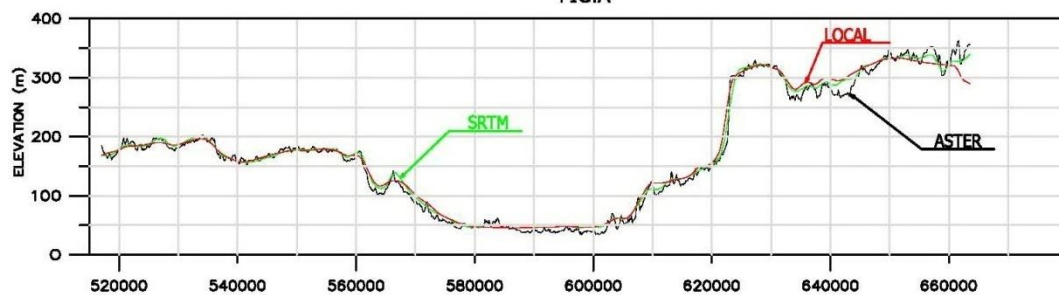
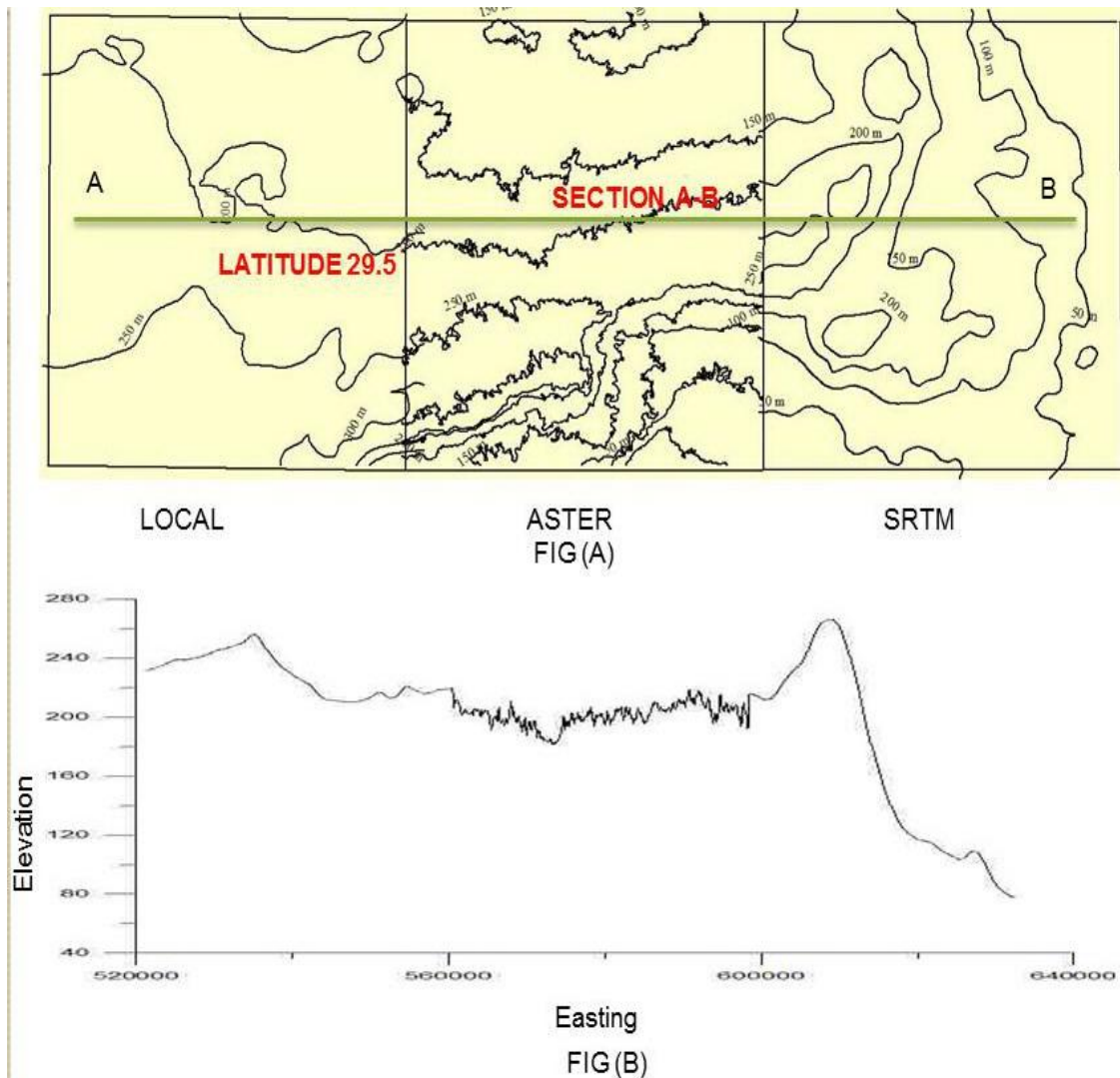


FIG:B

**Figure 4:** Profiles of DEMs; (a) before correcting ASTER DEM, and (b) after correcting ASTER DEM.

The derived contours and the profile of the three successive adjacent sectors of the original DEMs were shown in figures (5-A and 5-B). From these figures, one can note

that the DEMs contour lines aren't continues in these three adjacent DEMs. Also the middle part of the profile of the ASTER DEM seems lower than the other two DEMs on either sides. On the other hand, at figures (6-A and 6-B), there is a continuity in the contour lines along the adjacent sectors of the three DEMs and the middle part of the ASTER profile seems on the same level of the others two DEMs on either sides.



**Figure 5:** Derived contours; profiles of the original DEMs.

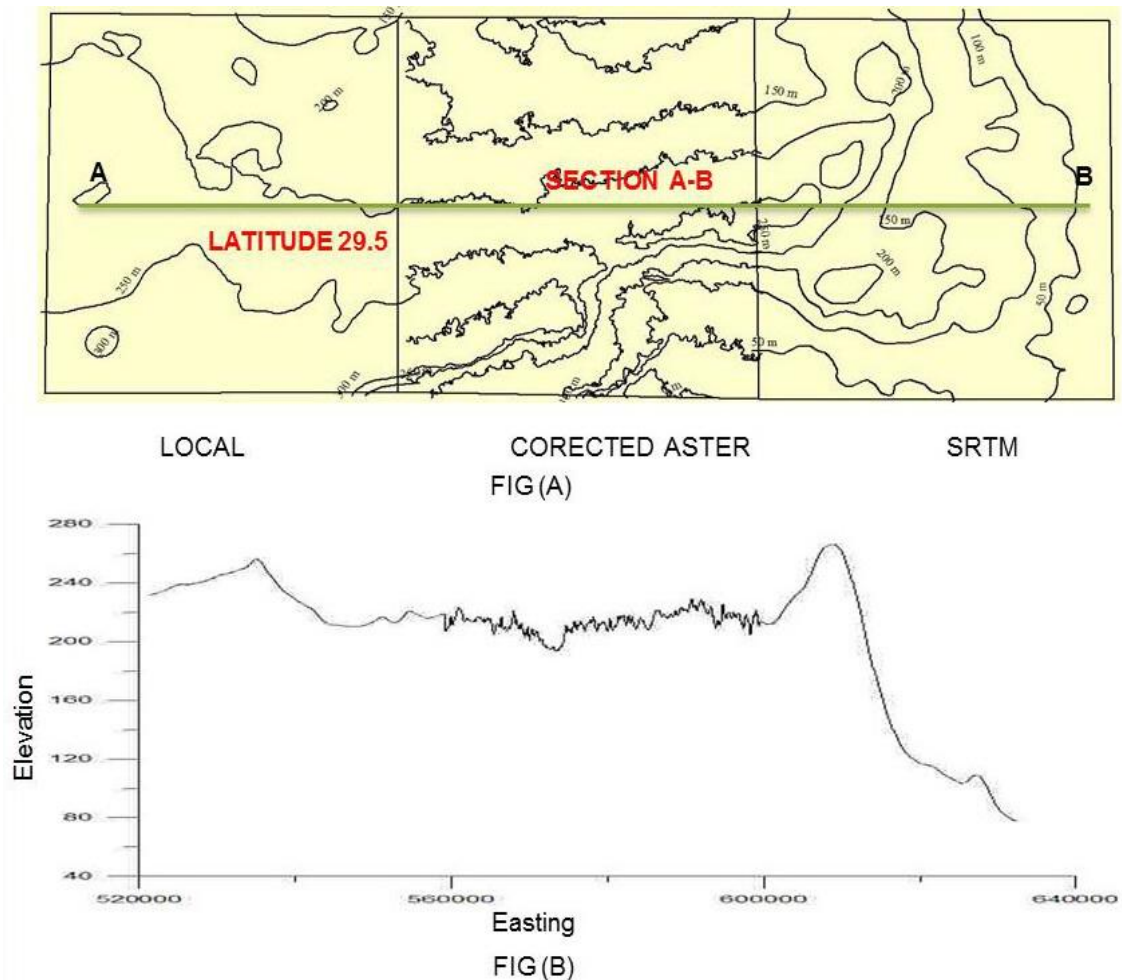


**Figure 6:** Derived contours; profiles of the corrected DEMs

After correcting ASTER DEM for the vertical and horizontal shifts, fusion among the three DEMs was made using different combination; a) ASTER + SRTM, b) SRTM + local DEM, c) ASTER + local DEM and finally d) ASTER + SRTM + local DEM. The fusion was performed for each combination using weighting averaging method. Because there are multiple elevation estimations of a resulted fused pixels, the weighted-average method through the surfer software is used to calculate the final fused DEM pixels, the fused DEM will have the smallest grid size. For example, if ASTER and SRTM DEMs will be incorporated in one fused DEM, the produced fused DEM will have a grid size of 30 m. Eight-neighborhood of each pixel will form a matrix

during a fusion. Weights were maintained in a weight matrix during the pixel fusion process. The weights were calculated with the following equation:

$$w = \frac{1}{\left(\frac{1}{n} \sum_{i=1}^n \frac{1}{w_i} + 1\right)} \quad (2)$$

While, the estimated elevation is given by the following equation:

$$h = \left( \frac{\sum_{i=1}^n w_i \cdot h_i}{\sum w_i} \right) \quad (3)$$

n : Number of reference points in the search area.

$W_i$ : The weight, which is a function of the distance (d)

The weight function  $W(d)$  can be taken as:

$$w_i = \frac{1}{d^2} \quad (4)$$

Where

$$d = \sqrt{(X - X_i)^2 + (Y - Y_i)^2} \quad (5)$$

Qualitatively, the DEM accuracy was improved due to the fusion process as can be ascertained from comparing fused DEM with the GCPs, see figures 7,8 and 9. The elevation difference between the fused DEM and reference data was almost invariably smaller than that of the individual DEMs. Also the fused DEM almost always lies between the reference data and the individual DEM, which give an indication of reliability of the fused DEM.

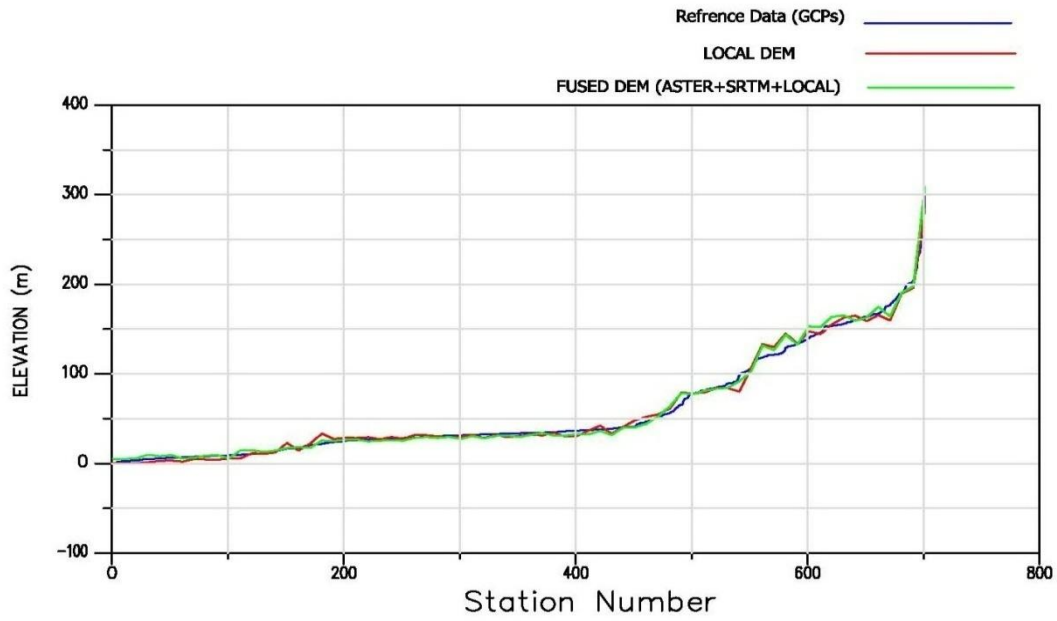


**Figure 7:** Relation between local DEM and the fused DEM at each GCP.

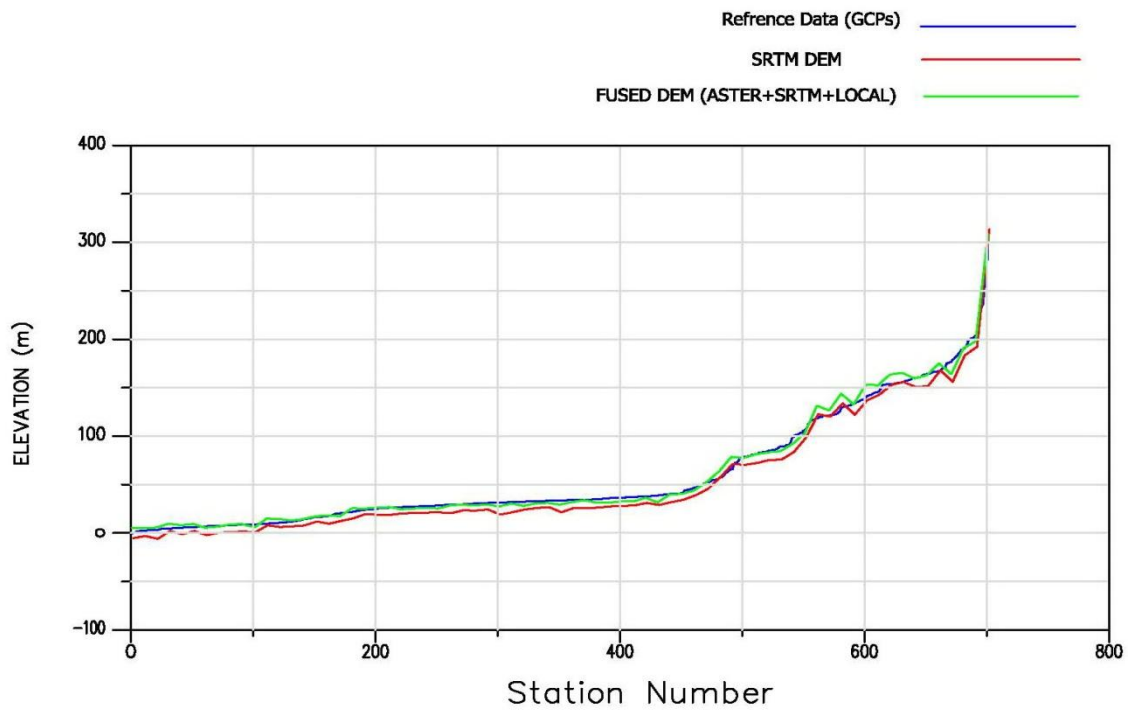


**Figure 8:** Relation between SRTM and the fused DEM at each GCP.

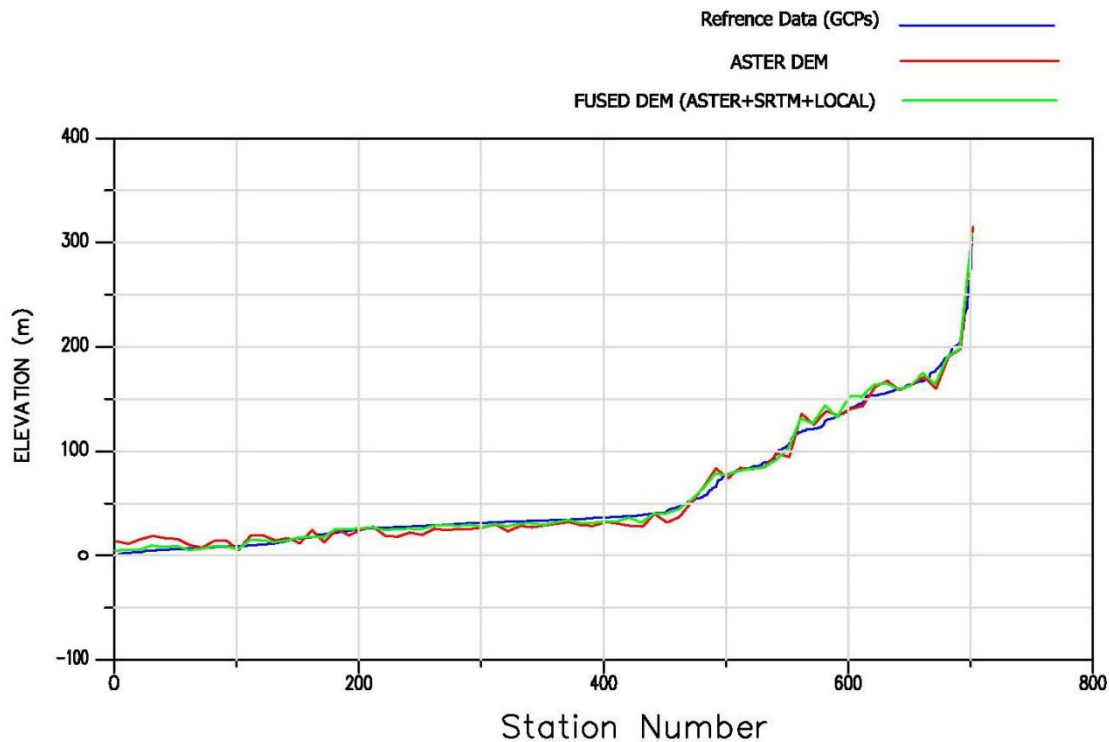


**Figure 9:** A relation between ASTER and the fused DEM at each GCP.

## 6 DEM Filtering.

The low-pass filtering is a popular filtration technique, it is used to remove the high frequencies from the fused DEMs. This technique is performed using surfer software. low-pass filter is also known as smoothing or blurring filter. This type of filter may cause ringing in the filtered image since it completely removes the frequency components beyond the average cut-off frequency [12]. It removes the high frequency noise with the resulting output being a smoother grid. Merging between any two DEMs needs suitable filtering techniques. A number of experiments were made to determine the filter technique which is more suitable for each case after merging, based on the resulted accuracy of the fused DEM. There are many user-defined low-pass filters. Each of these filters allows to specify the size of the neighborhood. A low pass filter using Gaussian 3 by 3 was the best technique suitable in our case for the four fused DEMs based on the resulted accuracy of the fused DEMs after applying the filtration.

The accuracies of the fused DEMs were significantly improved after fusion and filtration. Table (6) list the related statistics.

**Table (6):** Statistics of the fused and filtered DEMs over whole terrain.

DEMs	Z- difference, m			No of check points ( GCPs)	RMSE, m
	Min	Max	Mean		
ASTER plus SRTM	-14.46	15.76	1.34	705	4.95
SRTM plus local plus ASTER	-16.82	12.42	0.23	705	4.55
SRTM plus local	-17.62	16.31	0.79	705	4.21
ASTER plus local	-14.54	15.02	1.63	705	6.8

Since the fusion was applied to the 30 m-90 m and 200 m resolution input DEMs, the fused DEM had the least grid size of resolution of the four suits. These improvements in accuracy and completeness are vital to improve the reliability and thus the applicability of the produced DEMs. The improvement of DEMs accuracy after fusion and filtration were listed in the table (7).

**Table 7:** The accuracy improvement of DEMs due to fusion and filtration over whole terrain.

DEMs	RMSE/ after fusion	RMSE/after fusion and filtering	Improvement % due to filtration only	The Improvement% due to fusion and filtration
ASTER plus SRTM	6.62	4.95	26.22%	65%, -4.8%
SRTM plus LOCAL DEM plus ASTER	4.55	4.55	0.00%	6%, 3.6%, 68%
SRTM plus LOCAL DEM	4.66	4.21	14.70%	10%, 13%
ASTER plus LOCAL DEM	6.9	6.8	2.01%	53%, -40%

Figures (10A and 10B) show the derived contours and the profiles of the three successive adjacent sectors after fusion and filtering DEMs. There is a continuity in the contour lines along the adjacent sectors of the three DEMs, where, the middle part of the ASTER profile appears more smoothed and seems to have the same elevation of the others two DEMs on either sides.

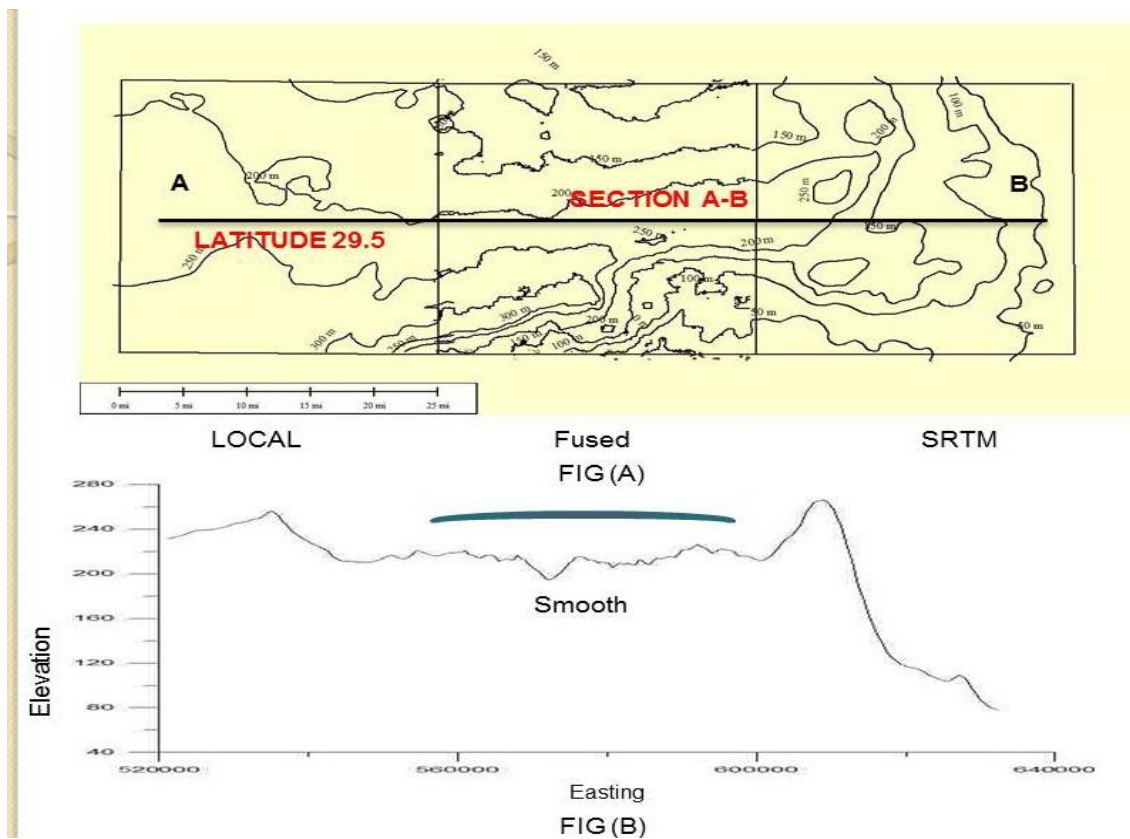


**Figure (10):**Derived contours; profiles of the final fused and filtered DEM.

## 7 Conclusions and Recommendations

### 7.1 Conclusions

Considering the results obtained in the previous sections it can be concluded that:

- SRTM and LOCAL DEM nearly has the same accuracy in terms of RMSE, while ASTER DEM less accuracy.
- The accuracy of the DEMs was improved after the vertical shifts versus GCPs have been removed especially in the case of the ASTER DEM.
- The vertical accuracy of the ASTER DEM was improved by 3.2% after co-registered to the local DEM
- The vertical accuracy of the ASTER DEM improves twice after correcting its horizontal position versus local DEM and eliminating its vertical shift versus SRTM DEM.



- For obtaining more reliable fused DEM it is essential to remove the horizontal and vertical shifts of the ASTER DEM.
- Fusion and filtration process yield a significant accuracy improvement especially in the case of integrating the data of the three DEMs.
- The fused DEM obtained from SRTM and ASTER DEMs only can be used for producing a reliable and accurate DEM, with sufficient data, to produce topographic maps of scale 1: 50,000 for regions having such topographic maps as the west desert of Egypt.

## 7.2 Recommendations

- Before using ASTER DEM elevation data, it is recommended to check the horizontal position of the ASTER DEM and correct it, if necessary, using some obvious features on the surface of the earth, like roads intersections.
- It is also recommended to determine and remove the vertical shift, if exists, using sufficient numbers of GCPs, distributed fairly in the interested area, to obtain good results.
- It is recommended to use the fused DEM obtained from SRTM and ASTER DEMs only, after make a necessary corrections and filterations, for producing a topographic maps of scale 1: 50,000 for regions having such topographic maps as the west desert of Egypt.

## 8 References

- [ 1 ] Amin, M.M.; El-Fatairy, S.M. and Hassouna, R.M. 2003: “A Digital Elevation Model for Egypt by Collocation” Scientific Bulletin of Matarya Faculty of Engineering, Helwan University, Cairo, Egypt.
- [ 2 ] Annamaria, C., et al., 2005: “Accuracy assessment of digital elevation model using stochastic simulation”, 7<sup>th</sup> international symposium on spatial accuracy assessment natural recourses and environmental science(2005).
- [ 3 ] Crosetto M; Crippa B 1998. “Optical and radar data fusion for DEM generation”. IAPRS, 32(4), 128–134
- [ 4 ] Caruso, V. 1987 : “ Standards for Digital Elevation Models ” , ASPRS - ACSM American Society for Photogrammetry and Remote Sensing and American Congress on Surveying and Mapping ,USA
- [ 5 ] Gonçalves, G.,2006.“Analysis of Interpolation Errors in Urban Digital Surface Models Created from Lidar Data”, 7th International Symposium on Spatial Accuracy Assessment in Natural Resources and Environmental Sciences, ed. M. Caetano and M. Painho, 2006, pp. 160–168
- [ 6 ] Honikel M., 1998.“Fusion of optical and radar digital elevation models in the spatial frequency domain”. Workshop on retrieval of Bio- And Geo-Physical Parameters From SAR Data For Land Applications, ESA-ESTEC, Oct 21–23, 1998. Remote Sensing of Environment, 94, 463–474.
- [ 7 ] Honikel M., 1999.“Strategies and methods for the fusion of digital elevation models from optical and SAR data”. In: IAPRS, 32, 7–4-3 W6, Jun 3–4, 1998, Valladolid, Spain.
- [ 8 ] InternetWebSite(2013):“GlobalElevation Datasets”,<http://worldwidescience.org/topicpages/a/aster/global/digital.html>.
- [ 9 ] Kaab A., 2005.“ Combination Of SRTM3 And Repeat ASTER Data For Deriving Alpine Glacier flow Velocities In The Bhutan Himalaya”. Remote Sensing of Environment, 94, 463–474.



[ 10 ] Liu et al., 2003; Seeker and Vachon, 2007:“Exploitation of multi-temporal SAR and EO satellite imagery for geospatial intelligence”. In: IEEE International Conference on Information Fusion, July 9–12, 2007, Quebec City, Canada.

[ 11 ] LANG, H. and WELCH, R., 1999:“Algorithm Theoretical Basis Document for ASTER Digital Elevation Models”. Standard Product AST14 Report, The Jet Propulsion Laboratory, California Institute of Technology, Los Angeles, CA.

[ 12 ] ManojKarkee, Brian L. Steward\*, SamsuzanaAbd Aziz., 2008. “ Improving Quality Of Public Domain Digital Elevation Models Through Data Fusion” Agricultural and Biosystems Engineering Department, Iowa State University, United States

[ 13 ] Qudus O. Taiwo and C. O. Adeofun, Nigeria., 2006. “Accuracy Assessment of Digital Terrain Model Data”: A Cost Effective and Analytical Approach Promoting Land Administration and Good Governance, 5th FIG Regional Conference. Accra, Ghana.

[ 14 ] Rabus B; Eineder M; Roth A; Bamler R 2003. “ The shuttle radar topography mission” – a new class of elevation model acquired by spaceborne radar. ISPRS Journal of Photogrammetry and Remote Sensing, 57(4), 241–262.

[ 15 ] Strozzi T; Wegmüller U; Wiesmann A; Werner C (2003). “Validation of the X-SAR SRTM DEM for ERS and JERS SAR geocoding and two pass differential interferometry in alpine regions”. In: IGARSS, July 21–25, 2003, Toulouse, France. Survey Department. (2004). Topographic BaseMaps of Nepal. Survey Department of the Government of Nepal, Kathmandu, Nepal.

[ 16 ] Taramelli, A. C., et al., 2005: “Comparison of SRTM elevation data with Cartographically derived DEMs in Italy”ICRAM, Marine Sciences Research Institute via di Casalotti, 300, Rome, ITALY

[ 17 ] Van Zyl, J.J., 2001. “The Shuttle Radar Topography Mission (SRTM) ”: a breakthrough in remote sensing of topography. Act Astrona. 48 (5-12), 559–565

[18] Wolf, 1987. “Elements of Photogrammetry”. McGraw-Hill, Inc. Singapore